

# Improving probes of $hAA$ coupling in the Type-X two Higgs Doublet Model scenario: the crucial role of $\tau$ -jet charge identification

Biswarup Mukhopadhyaya,<sup>\*</sup> Sirshendu Samanta,<sup>†</sup> Tousik Samui,<sup>‡</sup> and Ritesh K. Singh<sup>§</sup>

*Department of Physical Sciences,  
Indian Institute of Science Education and Research Kolkata,  
Mohanpur, 741246, India.*

## Abstract

The exotic decay modes of the already discovered 125-GeV scalar into a pair of light pseudoscalars is a good probe of those new physics scenarios where such pseudoscalars exist. Searches in the mass region where the pseudoscalar ( $A$ ) is lighter than 62.5 GeV have yielded null findings so far. No search has yet examined  $m_A > 62.5$  GeV where the cross section is suppressed by the off-shell pseudoscalar. We point out a possible enhancement of the sensitivity of probing  $hAA$  coupling in the context of a Type-X two Higgs doublet model. We focus on  $h \rightarrow AA^{(*)} \rightarrow 4\tau$ , and select events with two same-sign  $\tau$ -jets along with a pair of same-sign leptons. This enables much more effective background elimination than in the erstwhile proposed channels. Taking two values of the  $\tau\tau A$  coupling into account, we obtain limits on the  $hAA$  coupling that can be probed at  $2\sigma$  and  $3\sigma$  significance, for  $m_A$  ranging up to 85 GeV. For  $m_A < 62.5$  GeV, too, we find the probe through our suggested channel exhibits considerable improvement upon the usual  $2\mu 2\tau$ -based searches conducted at the LHC. Within this region, achieving the reach of  $\lambda_{hAA}$  coupling at  $3000 \text{ fb}^{-1}$  luminosity using our strategy would require approximately  $\sim 3.6 \times 10^5 \text{ fb}^{-1}$  luminosity using conventional  $2\mu 2\tau$ -based searches.

---

<sup>\*</sup> [biswarup@iiserkol.ac.in](mailto:biswarup@iiserkol.ac.in)

<sup>†</sup> [ss21rs027@iiserkol.ac.in](mailto:ss21rs027@iiserkol.ac.in)

<sup>‡</sup> [tousik.pdf@iiserkol.ac.in](mailto:tousik.pdf@iiserkol.ac.in)

<sup>§</sup> [ritesh.singh@iiserkol.ac.in](mailto:ritesh.singh@iiserkol.ac.in)

## I. INTRODUCTION

Although the Standard Model (SM) hypothesizes a single electroweak symmetry breaking  $SU(2)$  doublet, observed data allow the participation of other scalar multiplets [1–6]. Furthermore, the observed repetition of fermion families provides a spur to the idea of an extended electroweak symmetry-breaking sector. The first stride in this direction leads to two Higgs doublet models (2HDM), of which several types exist [1, 7–10]. These various types essentially differ from each other in the Yukawa interactions of the two doublets. The phenomenological constraints on the masses of the various spinless physical states depend on these Yukawa couplings since they affect production as well as decay channels, and also the role of these scalars in loop-induced rare processes. A question naturally arising, and of phenomenological interest, is: can the masses of some spin-zero particles [11–14] in certain kinds of 2HDM lie well below the 125-GeV scalar [15, 16] that has already been discovered?

The physical pseudoscalar state  $A$  in 2HDM is the readiest candidate here. This is because this state is more likely to be well-separated in mass from the heavier neutral scalar and the charged scalar, which are more constrained, in an inter-related manner, from collider searches [17], rare decays [18–20], and also electroweak precision measurement data [21, 22]. At the same time, a light pseudoscalar is phenomenologically viable when its coupling with quarks is suppressed [14, 23]. Out of the major 2HDM types, this is possible in the Type-X scenario, where one of the doublets couples to quarks only, and the other, only to leptons, engineered by an appropriate  $\mathbb{Z}_2$ -symmetry in the Yukawa sector.

The neutral pseudoscalar  $A$  in Type-X 2HDM has unsuppressed couplings with leptons only if the so-called ‘alignment limit’ has to be adhered to [2, 24, 25]. It is of obvious interest to look for it at the Large Hadron Collider (LHC) [26–28]. Moreover, it is useful to find out about the parameters of the scalar potential in such a scenario using data from the high-luminosity LHC (HL-LHC) [29–31]. For instance, the pseudoscalar pair produced in the decays of  $h$ , the 125-GeV scalar, is driven by the  $hAA$  interaction strength. In this work, we suggest new ways of extracting such information, using some features of the  $4\tau$  final state arising from  $h \rightarrow AA$ .

For the case where  $h \rightarrow AA$  is kinematically allowed, searches have been performed in the  $4\mu$  [32, 33],  $4b$  [34, 35],  $2b2\tau$  [36],  $2\mu2\tau$  and  $4\tau$  [37–41] channels at the LHC. These searches tend to disfavour a pseudoscalar lighter than  $m_h/2$ . Upper limits on the  $hAA$  interaction strength (depending, of course, on the other 2HDM parameters) are also obtainable. However, these limits pertain to on-shell production of both the  $A$ ’s in  $h$ -decay. With one  $A$  becoming off-shell, the usual

search channels get overridden by backgrounds, making studies at the HL-LHC difficult.

Two questions can be asked now: (a) Can the light pseudoscalar scenario be probed beyond  $m_A \geq m_h/2$ ? And (b) What are the ranges of the  $hAA$  interaction strength, which can be probed for various values of  $m_A$ , thus providing insight into the 2HDM scalar potential? We address both of these questions here and arrive at positive answers.

The special features of this work lie in the following points:

- We suggest looking for  $h \rightarrow AA^{(*)} \rightarrow 4\tau$  yielding final states where two same-sign  $\tau$ 's decay leptonically, while the two remaining ones (again of the same sign) undergo hadronic decay in one-prong and three-prong modes. One can then concentrate on signals consisting of two same-sign leptons plus a pair of same-sign  $\tau$ -jets. Given the recent estimates of  $\tau$ -jet charge identification efficiency [42], we show such signals, with appropriate cuts that we propose, to be significantly more effective in reducing backgrounds [21]. Thus, our event selection criteria make it possible to extend the probe of the  $hAA$  coupling strength well beyond the reach of strategies adopted earlier [37–41].
- The level at which the  $hAA$  interaction strength can be probed using the aforementioned signal depends also on the  $A\tau\tau$  Yukawa interaction strength since one is thinking here in terms of an off-shell  $A$  driving our signal. We thus benchmark our probes in terms of the  $A\tau\tau$  coupling strength. This gives further insight into the parameter space of the theory.

Incidentally, a low-mass pseudoscalar in Type-X 2HDM scenario has been often suggested as a solution [23, 43–49] to the deficit in  $(g-2)_\mu$  [50], the muon anomalous magnetic moment, predicted in the standard model (SM) [51]. However, claims from lattice estimates [52–62] of  $(g-2)_\mu$ , as well as mutually contradictory data-driven estimates [50, 63–65] of the hadronic vacuum polarisation contributions, make the scenario more fluid on this front. Our discussion in this paper is therefore dissociated from the  $(g-2)_\mu$  issue, and we treat the search for a light pseudoscalar as important by its own right.

The organization of the paper is as follows: a brief description of the Type-X 2HDM and parameter space limitations are discussed in Section II, which serves as the justification for using benchmark points. The methodology of our analysis has been discussed in Section III A, and the suggested signal, including the discussion of its backgrounds, is presented in Section III B. The results are then presented and examined in Section III C. We then summarize our work in Section IV.

## II. TYPE-X 2HDM: PARAMETERS AND CONSTRAINTS

The general framework of 2HDM extends the SM scalar sector by another  $SU(2)_L$  Higgs doublet with hypercharge same as the SM Higgs doublet. After the electroweak symmetry breaking (EWSB), the two doublets  $\Phi_1$  and  $\Phi_2$  receive their vacuum expectation values (vev)  $v_1$  and  $v_2$ , respectively. These two vevs are usually re-parametrized in terms of  $\tan \beta \equiv v_2/v_1$  and  $v \equiv \sqrt{v_1^2 + v_2^2}$ . As it involves two doublets, it is natural to have flavour-changing neutral current (FCNC) [66], for which no significant experimental evidence has been observed so far, to occur at the tree level after the EWSB. To avoid the FCNC, an extra symmetry, namely  $\mathbb{Z}_2$ , is usually imposed, and odd charges are assigned to  $\Phi_1$  and a set of right-handed fermions. Depending on this set, four different types of 2HDM occur. These four types are Type-I, Type-II, Type-X, and Type-Y (also called flipped type). A comprehensive discussion of these four types, including their phenomenological consequences, can be found in Ref. [1, 10]. With this  $\mathbb{Z}_2$  symmetry, the  $CP$ -conserving scalar potential can be written as:

$$\begin{aligned}
 V_{\text{scalar}} = & m_{11}^2 \Phi_1^\dagger \Phi_1 + m_{22}^2 \Phi_2^\dagger \Phi_2 + \lambda_1 \left( \Phi_1^\dagger \Phi_1 \right)^2 + \lambda_2 \left( \Phi_2^\dagger \Phi_2 \right)^2 + \lambda_3 \left( \Phi_1^\dagger \Phi_1 \right) \left( \Phi_2^\dagger \Phi_2 \right) \\
 & + \lambda_4 \left( \Phi_1^\dagger \Phi_2 \right) \left( \Phi_2^\dagger \Phi_1 \right) + \left\{ -m_{12}^2 \Phi_1^\dagger \Phi_2 + \frac{\lambda_5}{2} \left( \Phi_1^\dagger \Phi_2 \right)^2 + \text{h.c.} \right\}, \quad (1)
 \end{aligned}$$

Note that, although the quadratic term  $m_{12}^2 \Phi_1^\dagger \Phi_2$  violates  $\mathbb{Z}_2$  symmetry softly, it does not induce any further FCNC [67]. After the spontaneous breaking of the electroweak symmetry, three degrees of freedom are absorbed by the electroweak gauge bosons to receive their masses. The remaining modes appear as physical scalars as one pseudoscalar  $A$ , one charged scalar  $H^\pm$ , and two neutral  $CP$ -even scalars  $H$  and  $h$ . The mass matrices of the charged scalars and pseudoscalars are diagonalized by the same mixing angle  $\beta = \tan^{-1}(v_2/v_1)$ , while the diagonalization of the neutral  $CP$ -even scalar mass matrix requires a different angle, say,  $\alpha$ . For our study, we concentrate on a paradigm where  $h$  is identified as the observed 125-GeV scalar, the pseudoscalar is lighter than  $h$ , and other scalars are heavier than these two. This parameter region can be achieved by appropriately adjusting the six free parameters, namely  $\lambda_1, m_H, m_{H^\pm}, m_A, \tan \beta, m_{12}^2$  after redefining the Lagrangian parameters and setting the mass of  $h$  and the vev  $v$  to their respective observed values at 125 GeV and 246 GeV.

The constraint arises from the theoretical side to ensure the scalar potential remains bounded from below [68, 69], which gives the following conditions on the  $\lambda$  parameters.

$$\lambda_{1,2} > 0, \quad \lambda_3 > -\sqrt{\lambda_1 \lambda_2}, \quad \text{and} \quad \lambda_3 + \lambda_4 - |\lambda_5| > -\sqrt{\lambda_1 \lambda_2}.$$

The second source of theoretical constraints comes from the tree-level unitarity preservation [70, 71] in pure scalar-scalar elastic and inelastic scattering processes ( $S_1 S_2 \rightarrow S_3 S_4$ ) dominated by quartic interactions. From the mode partial wave decomposition of the scattering amplitudes, this unitarity constraint can be extracted from the condition  $\Re(a_l)^2 + \Im(a_l)^2 = |a_l|^2 = \Im(a_l)$ , where  $a_l$  is the  $l^{\text{th}}$  mode of partial wave. In graphical representation, this constraint, in turn, puts  $|\Re(a_l)| < \frac{1}{2}$ . These theoretical constraints put restrictions on the parameter space, details of which can be found in Ref. [70]. Furthermore, to have a perturbative Lagrangian, the quartic couplings should obey  $|\lambda_i| < 4\pi$ , ( $i = 1, 2, \dots, 5$ ). We have verified that the parameter points chosen for further analysis satisfy these constraints.

In this work, we focus on the Type-X scenario, in which the lepton Yukawa coupling is with the doublet  $\Phi_1$ , and quark Yukawa couplings are with the doublet  $\Phi_2$ . With these charge assignments, the Yukawa coupling after the EWSB becomes

$$\begin{aligned} \mathcal{L}_{\text{Yukawa}} = & - \sum_f \frac{m_f}{v} \left( \xi_f^h \bar{f} f h + \xi_f^H \bar{f} f H - i \xi_f^A \bar{f} \gamma_5 f A \right) \\ & - \sum_{u,d} \frac{\sqrt{2}}{v} \left[ V_{ud}^{\text{CKM}} (m_u \xi_u^A \bar{u}_R d_L + m_d \xi_d^A \bar{u}_L d_R) H^+ + m_\ell \xi_\ell^A \bar{\nu}_L \ell_R H^+ + \text{h.c.} \right], \end{aligned} \quad (2)$$

where

$$\begin{aligned} \xi_{u,d}^h &= \frac{\cos \alpha}{\sin \beta}, & \xi_{u,d}^H &= \frac{\sin \alpha}{\sin \beta}, & \xi_{u,d}^A &= \pm \cot \beta, \\ \xi_\ell^h &= -\frac{\sin \alpha}{\cos \beta}, & \xi_\ell^H &= \frac{\cos \alpha}{\cos \beta}, & \xi_\ell^A &= \tan \beta. \end{aligned} \quad (3)$$

As a phenomenological consequence, mainly dictated by the Yukawa coupling of the top quark, one needs to take large  $\tan \beta$  in this setup. The experimental observations, mainly the resemblance of the 125-GeV scalar to the SM Higgs boson, sets  $\beta - \alpha \simeq \pi/2$ , which is the so-called ‘alignment limit’. In this large  $\tan \beta$  and alignment limit, Type-X 2HDM shows an interesting scenario where new scalars, namely  $H^\pm$ ,  $A$ , and  $H$ , couple feebly to the quarks but strongly couple to the leptons. This has consequences, especially in the low  $m_A$  region, in generating large new physics contributions to  $(g-2)_\mu$ , in which a significant excess is seen in the BNL [72] and FNAL [50] experiments. There are ongoing debates about whether or not this excess really exists since fresh calculations of the SM prediction indicate otherwise [59, 65]. Nevertheless, this large coupling of  $A$  to lepton plays an important role in our study since we are also interested in the  $h \rightarrow AA \rightarrow 4\tau$  channel. This is because the Yukawa coupling in Eq. (2) between the pseudoscalar and leptons has an enhancement factor  $\tan \beta$ , and, due to the highest mass of  $\tau$  lepton, the dimensionless  $y_{\tau\tau A}$  coupling is dominant in the alignment limit. So, the primary decay mode of the pseudoscalar is in the  $\tau$  channel ( $\sim 100\%$ ).

One source of the constraints on the model parameters comes from the measurement of the properties of the observed 125-GeV scalar. Although the observed scalar mostly resembles the SM Higgs boson, it still leaves a tiny window to keep our model parameters. We have performed a thorough study of these constraints, primarily in the measurement of Higgs signal strength, defined as the ratio of the production cross section of the 125-GeV scalar in a particular channel to the SM prediction of that. For this, we used `HiggsSignals` [73] which is implemented within the package `HiggsTools` [74]. The second experimental constraints come from the search for other scalars for which we do not have a clear signal, and thus, the cross sections of the production of these other scalars ( $H^\pm$ ,  $H$ , and  $A$  in our model) is measured to be less than the detectable values. These searches have been performed in the Large Electron-Positron (LEP) collider and in the LHC in the  $h \rightarrow AA$  [34, 36, 39, 40, 75, 76],  $H \rightarrow ZZ/W^+W^-$  [77–79],  $H \rightarrow hh$  [80–82] etc. channels. We have used `HiggsBounds` [83] using `HiggsTools` [74] to verify the validity of the model parameters at 95% C.L.

The other set of constraints comes from the measurement of electroweak precision observables (EWPO), which are defined through Peskin-Takeuchi electroweak oblique parameters,  $S$ ,  $T$  and  $U$  [84]. These observables have been measured with good precision at the LEP [85]. For new physics, the values of specified parameters deviate from the standard model’s value, which is exactly zero. The parameter  $U$  can be taken as zero due to having a suppression factor compared to  $S$  and  $T$ . We have taken the current best-fit result,  $S = -0.01 \pm 0.07$ , and  $T = 0.04 \pm 0.06$  in the limit  $U = 0$  [86]. All the parameter points we consider are inside the 90% C.L. contour in the  $S - T$  plane.

### III. COLLIDER STUDY

#### A. Analysis Methodology

We are interested in the search of pseudoscalar ( $A$ ) in  $h \rightarrow AA$  channel in the gluon-gluon fusion (ggF) production of the  $h$ . In our model, the  $hgg$  coupling resembles the SM values in the high  $\tan\beta$  and alignment limit. So, the coupling that can be probed in this channel is the coupling  $\lambda_{hAA}$ , the coupling between the Higgs boson  $h$  and the pseudoscalar  $A$ . In terms of the other parameters of the theory, this coupling takes the following form in the alignment limit:

$$\lambda_{hAA} \approx v \sin^4\beta (\lambda_3 + \lambda_4 - \lambda_5). \quad (4)$$

This non-zero coupling  $\lambda_{hAA}$  contributes to the branching ratio (BR) of  $h$  to its non-standard decays whenever  $m_A < m_h/2$ . The expression for the BR in this mode can be written as

$$\text{BR}(h \rightarrow AA) = \frac{\Gamma(h \rightarrow AA)}{\Gamma_h^{\text{SM}} + \Gamma(h \rightarrow AA)}, \quad (5)$$

where  $\Gamma_h^{\text{SM}}$  is the decay width of  $h$  to SM modes and the partial decay with for the decay  $h \rightarrow AA$  takes the form

$$\Gamma(h \rightarrow AA) = \frac{1}{32\pi} \frac{\lambda_{hAA}^2}{m_h} \sqrt{1 - \frac{4m_A^2}{m_h^2}}. \quad (6)$$

The partial decay widths of  $h$  to SM modes ( $\Gamma_h^{\text{SM}}$ ) remain almost unaltered with respect to those of the SM Higgs boson. This is because the fermion coupling modifiers  $\xi_{u,d,\ell}^h$  in Eq. (3) remain almost unity in the alignment limit. In this limit, the  $hWW$  and  $hZZ$  coupling modifiers, which take the form  $\sin(\beta - \alpha)$ , also remain close to one [1]. Therefore, for our analysis, we have used the value of  $\Gamma_h^{\text{SM}}$  as recommended by the LHC Higgs Cross Section Working Group (LHCHCSWG) [87–91], which uses the package HBDECAY [92, 93] to calculate the widths and branching ratios for all kinematically allowed channels, incorporating higher-order corrections. The calculation considers all relevant decay channels for the Standard Model Higgs boson, including  $h \rightarrow f\bar{f}$ , ( $f = t, b, c, \tau, \mu$ ),  $h \rightarrow VV$ , ( $V = g, \gamma, W, Z$ ), and  $h \rightarrow Z\gamma$ . Additionally, in the LHCHCWG calculations, the Monte Carlo event generator PropHECY4F [94–96] is also used to provide the partial widths for all possible four-fermion final states originating from  $h \rightarrow ZZ$  and  $h \rightarrow WW$  at both leading order (LO) and next-to-leading order (NLO).

The exotic decay of observed 125 GeV Higgs has been searched in various channels through pseudoscalars and yielded null results so far at the LHC. Searches have been performed in the  $4\mu$  [32, 33],  $4b$  [34, 35],  $2b2\tau$  [36],  $2\mu2\tau$  or  $4\tau$  [37–41] channels. However, since the pseudoscalar  $A$  is quark-phobic and dominantly decays to the leptons,  $4b$ ,  $2b2\tau$  channels are not at all sensitive in the context of Type-X 2HDM. The  $4\mu$  channel is also not sensitive compared to  $2\mu2\tau$  channel as the  $\text{BR}(A \rightarrow \mu\mu)$  is suppressed by a factor  $m_\mu^2/m_\tau^2$  compared to the  $\text{BR}(A \rightarrow \tau\tau)$ . Thus, the most sensitive channel, in principle, becomes  $4\tau$ . However, the  $\tau$ 's detected in their hadronic modes make the sensitivity of the search comparable to  $2\mu2\tau$  channel. Importantly, all the prior searches have been carried out in the region where the pseudoscalar mass is less than 62.5 GeV, where it is produced on-shell.

Our primary attempt is to extend the search beyond the on-shell region, *i.e.* to consider the pseudoscalar mass greater than 62.5 GeV. In other words, whether or not the search for  $h \rightarrow AA^*$ , where  $A^*$  represents the off-shell pseudoscalar, decay mode can be studied, and a potential signal

can be observed. The primary obstacle to probing beyond the 62.5 GeV mass zone is the extremely low number of signal events (even at  $100 \text{ fb}^{-1}$  of integrated luminosity) due to the presence of off-shell pseudoscalar and the overwhelming amount of background events. We, therefore, selected the dominant pseudoscalar decay mode through  $\tau$ -pairs to enhance the signal events considering HL-LHC in the future. The signal with  $4\tau$ 's has been tackled in the following way to suppress the background.

The  $\tau$  has two decay modes, *viz.* leptonic ( $\approx 35\%$ ), hadronic ( $\approx 65\%$ ) decay modes. The  $\tau$ , via its hadronic decay mode, is detected as a jet, called  $\tau$ -jet or  $\tau_h$ . The  $\tau$ -jets can be tagged with an efficiency of  $\approx 60\%$  as these are low multiplicity jets. When folded with the respective branching ratios, one expects the  $\tau$  can be identified at a rate of  $\approx 40\%$  in the hadronic mode, which is higher than its leptonic decay modes. However, the main difficulty comes in managing the SM QCD multijet and  $t\bar{t}$  backgrounds for which one expects billions of events in the HL-LHC. Although the misidentification rate of a QCD jet tagged as a  $\tau$ -jet is as low as 1.0%, due to the huge number of events, the SM background remains present with a significant amount. Thus, we look for the signals where two same-sign  $\tau$ 's decay leptonically and two same-sign  $\tau$ 's decay hadronically. This is possible because of the high efficiency in the charge identification efficiency of  $\tau$ -jets. These efficiencies are as high as 99% and 70% in the one-prong and three-prong decay, respectively [42]. On the other hand, the reconstruction efficiencies of the muons and electrons are very high, more than 97% [97, 98]. For those reasons, we kept two same-sign leptons and two same-sign  $\tau$ -jets as our main focus in the final states.

The same search strategy can be applied to the on-shell region, where ATLAS and CMS already set upper limits on the product of the cross section of  $pp \rightarrow h$  and  $\text{BR}(h \rightarrow AA)$ . In our study, we, however, probe for  $\lambda_{hAA}$  coupling instead of the  $\text{BR}(h \rightarrow AA)$  since we look into the off-shell region as well. In the off-shell region, the cross section of  $pp \rightarrow h \rightarrow AA^* \rightarrow 4\tau$  has a dependency on the actual value of the decay width of  $A$  through the Breit–Wigner. This effect is usually not present in on-shell decay mode, especially in the narrow width approximation, where Breit-Wigner contribution can be replaced by production cross section times the branching ratio. Therefore, the probe of  $\lambda_{hAA}$  coupling will depend on the value of decay width, which is primarily controlled by the Yukawa coupling  $y_{\tau\tau A}$ . Hence, we expect our probe of  $\lambda_{hAA}$  coupling to be less sensitive to  $y_{\tau\tau A}$  in the on-shell case and more sensitive to  $y_{\tau\tau A}$  in the off-shell case.

For our study, we have selected the pseudoscalar mass range between 40 GeV and 85 GeV. We primarily divide this selected  $m_A$  range into three regions, and we call them (a) on-shell region, (b) intermediate region, and (c) off-shell region. The first region is the on-shell region ( $40 \leq m_A < 60$ ),



where 125 GeV Higgs decays into two on-shell pseudoscalars, followed by their decay to  $\tau$ 's. In this region, the number of signal events is insensitive to the exact value of  $y_{\tau\tau A}$  coupling because the pseudoscalars are produced on-shell and the  $y_{\tau\tau A}$  coupling mainly contributes to the  $\text{BR}(A \rightarrow \tau\tau)$ , which is almost 100%. In the second region ( $60 \leq m_A \leq 65$ ), the 125 GeV starts decaying through one on-shell and one off-shell pseudoscalars. Hence, the corresponding event rate is highly sensitive to the decay width of the pseudoscalar. Therefore, the number of signal events becomes sensitive to the value of  $y_{\tau\tau A}$  coupling. Lastly,  $h$  decays mostly through one on-shell and one off-shell pseudoscalar in the third region ( $65 < m_A \leq 85$ ), with a little lower sensitivity to the  $y_{\tau\tau A}$  coupling than in the preceding regions.

To investigate the couplings in this study, we have taken a few discrete pseudoscalar masses and performed the analysis at those discrete mass points. Additionally, the cross section in the  $4\tau$  channel is sensitive to the actual value of the decay width of the pseudoscalar  $A$ , especially in the intermediate and off-shell regions. We thus take two different values of  $y_{\tau\tau A}$  coupling in the analysis. The mass points are chosen sparsely with a gap of 2.5 GeV in the on-shell region since the cross section is less sensitive to  $m_A$  in this region. However, in the intermediate region, the cross section is sensitive to the exact mass values. Hence, in this region, the mass points are chosen with a finer spacing of 0.5 GeV. In the off-shell region, the mass points are chosen with a spacing of 2.5 GeV again.

## B. Signal and Background

We took the dominant channel (ggF) for 125 GeV Higgs production, through which two pseudoscalars are produced, followed by decaying into  $4\tau$ 's, due to having almost 100% branching ratio in the di-tau mode. In addition, the cross section of the  $h$  production is significant in the one extra jet channel, where this extra jet appears due to initial state radiation (ISR). So, the signal topology, in which we are interested, is the production of  $h$  plus up to one extra jet. The process can be written as

$$pp \rightarrow h + (j) \rightarrow AA^{(*)} + (j) \rightarrow 2\tau^\pm + 2\tau^\mp + (j), \quad (7)$$

where, by  $A^{(*)}$ , we mean on-shell  $A$  or off-shell  $A^*$  depending on the region of our analysis.

The  $(2l^\pm + 2\tau_h^\mp)$  final state may arise from other sources that resemble our intended signal process. Although vector bosons predominantly contribute to the leptons and  $\tau$ 's production, they can originate from other places also, like the semileptonic decays of the  $B$ -hadrons. Furthermore, a

major challenge arises from the QCD jets, which can be misidentified as  $\tau$ -jets, while the misidentification of muons and electrons is insignificant. Considering all these, we list all potential sources of backgrounds below.

$$pp \rightarrow VV + (j), \quad (8)$$

$$pp \rightarrow t\bar{t}V, \quad (9)$$

$$pp \rightarrow t\bar{t} + (j), \quad (10)$$

where  $V$  represents vector bosons:  $Z$ , and  $W^\pm$  bosons. In the first process, four  $\tau$ 's can directly arise from the decays of the two vector bosons and can be regarded as irreducible backgrounds if both of them are  $Z$  bosons. In scenarios involving one  $Z$  boson and one  $W$  boson, leptons can arise through  $Z$  boson, while one  $\tau_h$  originates from  $W$  boson, and the extra QCD jet could be misidentified as a  $\tau$ -jet. This background contributes very little to the actual signal topology since two leptons are oppositely charged and the same-sign dilepton pair appears only due to the misidentification of the charge of one of the two leptons. The background for two  $W$  bosons is negligible because it requires a QCD jet to be misidentified as a lepton, and the other lepton and one  $\tau_h$  can come from  $W$  bosons, whereas second  $\tau_h$  would, again, have to come from a misidentified QCD jet. In the background process  $pp \rightarrow t\bar{t}V$ , the top quark has 100% decay into a bottom quark and a  $W$  boson, leaving  $b\bar{b}W^+W^-V$  as the hard process. This process has various combinations for misidentifying leptons and  $\tau_h$ 's. For instance, in the case of  $V = W$ , if two out of three  $W$  bosons undergo hadronic decay, one lepton can arise from the remaining  $W$  boson while another may originate via semileptonic decay of  $B$ -hadron. Similarly, one  $\tau_h$  can also be produced via  $B$ -hadron when the QCD jet is mistakenly detected as another  $\tau_h$ . Likewise, the third process  $pp \rightarrow t\bar{t} + (j)$  yields  $b\bar{b}W^+W^- + (j)$  as the hard process. Further, if one  $W$  boson decays hadronically, two leptons can arise from one  $W$  boson and one  $B$ -hadron. The other  $B$ -hadron could generate one  $\tau_h$ , while the other  $\tau_h$  might come as a result of misidentification of a QCD jet.

For the event generation, we have used the Mathematica-based package SARAH [99] to generate the UFO model file. The spectrum files have been generated from the SPheno [100] package, which calculates the Higgs masses, all types of couplings, decay widths, branching ratios, etc. All the signals and backgrounds have been simulated at the parton level at a centre-of-mass energy of 14 TeV using the well-known package, MadGraph5\_aMC@NLO [101]. Further showering and hadronization have been done through PYTHIA8 [102] followed by Delphes [103] for detector simulation. Jets are clustered using the anti- $k_t$  algorithm [104] with a radius of 0.5 GeV. As we have an additional jet, which has a chance to get generated at the hard process level as well as a result of parton

showering, in the final state, we have used the standard practice of Matching and Merging [105] through MadGraph5\_aMC@NLO and PYTHIA8 to eliminate the double-counting of the contribution of the events in the common phase space. All the background events have been generated at the leading order (LO). We have then used corresponding  $k$ -factors of the next-to-leading order (NLO) to scale the cross sections. The  $k$ -factors are 1.38, 1.57, 1.60, and 2.01, 1.72 for  $t\bar{t}Z$  [106],  $t\bar{t}W$  [107],  $t\bar{t}$  [108],  $\tau^+\tau^-W + \text{jets}$  [109], and  $2\tau^\pm + 2\tau_h^\mp + \text{jets}$  [110], respectively.

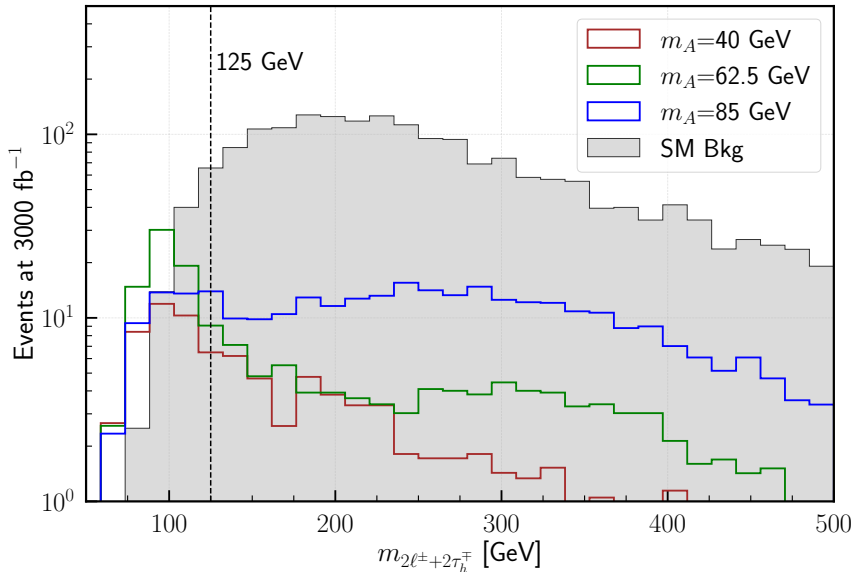


FIG. 1: Distribution of the invariant mass of  $(2\ell^\pm + 2\tau_h^\mp)$  for background (shaded) and signal for different pseudoscalar masses  $m_A = 40$  GeV (blue), 62.5 GeV (red), and 85 GeV (green). The parameters corresponding to the three pseudoscalar masses are given in Table I.

Regarding the distinctive features of the signal process, the key characteristic is all  $\tau$ 's are coming from 125 GeV Higgs, so at the parton level, their invariant mass would sharply peak around the Higgs mass. Furthermore, due to the missing neutrinos from the decays of  $\tau$ 's, the invariant mass tends to shift towards lower values as the final state contains  $(2\ell^\pm + 2\tau_h^\mp)$  with six missing neutrinos. The invariant mass ( $m_{2\ell^\pm+2\tau_h^\mp}$ ) distribution of these four objects is shown in Fig. 1 for three different  $m_A$  values and the corresponding parameters are given in Table I.

Depending on the  $\lambda_{hAA}$  and  $y_{\tau\tau A}$  couplings, the peak height would be different. Note that there is another wider bump that appears around 300 GeV in the signals, which come from the presence of other couplings that produce the same final states, *i.e.*  $4\tau + (j)$  but without  $h$  being present in the  $s$ -channel resonance. On the other hand, the backgrounds, especially the dominant  $ZZ$  and  $t\bar{t}$

Parameters	Benchmark Points		
	$m_A = 40$	$m_A = 62.5$	$m_A = 85$
$\lambda_1$	0.09	0.10	0.27
$\lambda_2$	0.13	0.13	0.13
$\lambda_3$	4.60	3.73	2.37
$\lambda_4$	-2.27	-1.90	-1.44
$\lambda_5$	2.32	1.84	1.12
$m_{12}$ (GeV)	41.44	37.26	30.01
$\tan\beta$	83.10	83.10	83.10
$m_A$ (GeV)	<b>40.00</b>	<b>62.50</b>	<b>85.00</b>
$\lambda_{hAA}$ (GeV)	<b>0.27</b>	<b>0.91</b>	<b>45.99</b>
$y_{\tau\tau A}$	<b>0.60</b>	<b>0.60</b>	<b>0.60</b>

TABLE I: The parameter points for different pseudoscalar masses used in Fig 1 to discriminate signal and background. The parameters  $m_A$ ,  $\lambda_{hAA}$  and  $y_{\tau\tau A}$  are dependent parameters.

backgrounds, tend to have the four-object invariant mass at a higher ( $> 150$  GeV) value. Therefore, in the final selection, we used an upper cut on  $m_{2\ell^\pm+2\tau^\mp}$ , which suppresses the backgrounds and eliminates contributions from diagrams without  $h$  in the  $s$ -channel. To discriminate signals from the backgrounds, we used the following important cuts:

$$p_T^{j_1} \geq 25 \text{ GeV}, \quad p_T^{\ell_1} \geq 15 \text{ GeV}, \quad m_{2\ell^\pm+2\tau^\mp} \leq 100 \text{ GeV}, \quad (11)$$

where  $p_T^{j_1}$  and  $p_T^{\ell_1}$  are the transverse momentum of the leading jet and the leading lepton.

### C. Results and Discussions

To start with the findings, we concentrate our efforts on the three areas mentioned. That is to say, we searched the collider signature of the pseudoscalar in the intermediate and off-shell region, where the pseudoscalar mass is larger than half of  $m_h$  ( $m_A \geq \frac{m_h}{2}$ ). We further investigated whether our approaches yield better results on the  $\text{BR}(h \rightarrow AA)$  than the earlier searches at the LHC [39] in the region where pseudoscalar mass is less than half of the mass of  $h$ . For this, we first calculate the significance  $\mathfrak{S}$  for a given value of  $\lambda_{hAA}$ . Given the number of signal events  $S$  and number of background events  $B$  after the final selection cut, one usually calculates the significance of discovering the signal. In the presence of relative systematics uncertainty  $\epsilon$ , the significance can

be calculated using the following formula.

$$\mathfrak{S} = \sqrt{2} \left[ (S + B) \ln \left( 1 + \frac{S}{B + \epsilon^2 B(S + B)} \right) - \epsilon^{-2} \ln \left( 1 + \frac{\epsilon^2 S}{1 + \epsilon^2 B} \right) \right]^{\frac{1}{2}}, \quad (12)$$

We then provide the discovery limit of potentially observing the signal at two specific values of signal significance, *viz.*  $2\sigma$  and  $3\sigma$  in Fig. 2. The blue dotted and black solid lines represent the values of  $\lambda_{hAA}$  for which the signal could be observed at  $2\sigma$  for  $y_{\tau\tau A} = 0.55$  and  $0.80$ , respectively. The green dash-dotted and red dashed lines represent the curves at  $3\sigma$  for the above two values of  $y_{\tau\tau A}$ . The two panels, *i.e.* Figures 2(a) and 2(b) correspond to the discovery limits of  $\lambda_{hAA}$  couplings assuming  $1000 \text{ fb}^{-1}$  and  $3000 \text{ fb}^{-1}$  luminosity, respectively. In all the curves, signal significance is calculated considering a moderate 10% systematics uncertainty. The essential features of the discovery limits can be noted down as follows

- The numerical value of the discovery limits of  $\lambda_{hAA}$  at  $3\sigma$  is larger than that at  $2\sigma$  since the former sets a higher level of signal significance and hence can only probe large values.
- In the on-shell ( $m_A < m_h/2$ ) region, the limit is almost insensitive to the actual value of  $y_{\tau\tau A}$  since both pseudoscalars are produced on-shell, and then each decays into a pair of  $\tau$ 's. The branching ratio of  $A \rightarrow \tau\tau$  is almost 100% and does not depend on the exact value of  $y_{\tau\tau A}$  in this parameter region.
- In the off-shell ( $m_A > m_h/2$ ) region, where one pseudoscalar is produced off-shell, the limit is dependent on the value of  $y_{\tau\tau A}$ . This is because the larger value of  $y_{\tau\tau A}$  coupling makes the decay width of the pseudoscalar larger, which contributes to higher di- $\tau$  production from an off-shell  $A$ . Higher production implies that the signal can be probed deeper, and hence, the discovery limit can be set to a smaller value. This can be seen in Figs. 2(a) and 2(b) where the two curves corresponding to  $y_{\tau\tau A} = 0.80$  sets stronger limits than the two lines corresponding to  $y_{\tau\tau A} = 0.55$ .
- Finally, higher integrated luminosity means being able to probe smaller values of  $\lambda_{hAA}$ . This feature is demonstrated in the figure, where one can see that each curve in Fig. 2(b) is shifted downward below with respect to the corresponding curve in Fig. 2(a). However, the systematics, which has been taken to be 10% in this analysis, tends to reduce the difference between the two cases.

Since no pseudoscalar search for masses greater than 62.5 GeV is reported in the available literature, our proposed methods of finding such signals in the two same-sign dilepton and two

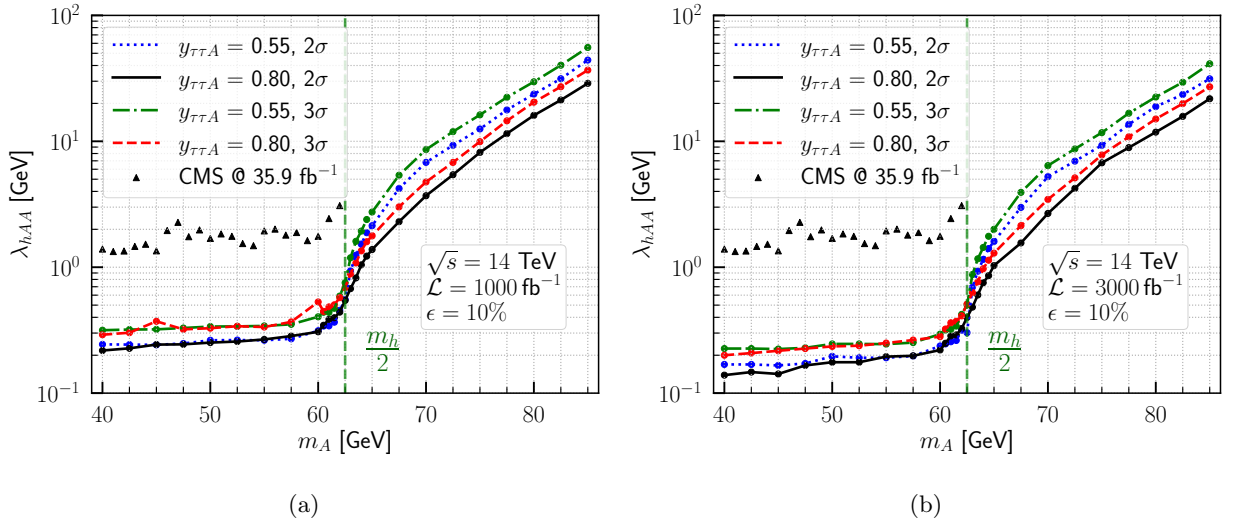


FIG. 2: Discovery limit of  $\lambda_{hAA}$  coupling as a function of  $m_A$  at  $2\sigma$  and  $3\sigma$  at different values of the dimensionless coupling  $y_{\tau\tau A}$ . The limits have been calculated with integrated luminosity (a)  $1000 \text{ fb}^{-1}$ , and (b)  $3000 \text{ fb}^{-1}$  with a moderate 10% systematic uncertainty at a centre-of-mass energy of 14 TeV LHC. The black triangle points represent the upper bound on the  $\lambda_{hAA}$  coupling in Type-X 2HDM, determined from observed data at CMS [39] with a 95% confidence level at an integrated luminosity of  $35.9 \text{ fb}^{-1}$  at 13 TeV LHC.

same-sign  $\tau$ -jets will help in the probe of  $\lambda_{hAA}$  couplings in the HL-LHC. On the other hand, the searches of  $h$  decaying to a pair of pseudoscalars have been performed in the region where the pseudoscalar mass is less than half of the mass of  $h$  at CMS in 2017 at  $19.7 \text{ fb}^{-1}$  of integrated luminosity [38]. Further, a follow-up search in 2018 at  $35.9 \text{ fb}^{-1}$  integrated luminosity improved the limit on the branching ratio by more than a factor of two [39]. In these searches, an upper limit on the branching ratio of  $h \rightarrow AA$  has been set at 95% C.L. in the  $2\mu + 2\tau_h$  channels, considering one pseudoscalar to decay to two  $\mu$ 's and the other to decay to two  $\tau$ 's. Hence, in these searches, both the  $\mu$  pair are required to have opposite signs, and the same for the  $\tau_h$  pair. The ratio of BRs in the  $\mu$  mode to  $\tau$  mode is assumed to be  $m_\mu^2/m_\tau^2$ . Assuming this ratio, one can get the upper limit on  $\text{BR}(h \rightarrow AA)$ . We then used the Eqs. (5) and (6) to obtain a limit on  $\lambda_{hAA}$ . The black triangle points in Fig. 2 represent the current upper limit on  $\lambda_{hAA}$  calculated from the upper limit on the  $\text{BR}(h \rightarrow AA)$  provided by the previous search in CMS at  $35.9 \text{ fb}^{-1}$  [39].

One might ask how our proposed analyses, which are performed assuming  $1000 \text{ fb}^{-1}$  or  $3000 \text{ fb}^{-1}$  luminosity, fair against the CMS analysis at  $35.9 \text{ fb}^{-1}$ . We explain this in the following way. At

integrated luminosity  $\mathcal{L}$ , the signal significance for  $h \rightarrow AA$  is proportional<sup>1</sup> to  $\lambda_{hAA}^2 \times \sqrt{\mathcal{L}}$  if we consider no systematics and the naive  $S/\sqrt{B}$  formula. Now, if  $\lambda_{hAA}$  becomes the observed limit at luminosity  $\mathcal{L}_0$ , one might simply estimate that the required luminosity to probe a coupling  $\frac{\lambda_{hAA}}{\alpha}$  ( $\alpha$  being a scale factor) would be  $\alpha^4 \mathcal{L}_0$ . Observing that the projected discovery limit of  $\lambda_{hAA} \approx 0.1$  GeV at  $3000 \text{ fb}^{-1}$  in our proposed channel is almost an order of magnitude better than the CMS result at  $35.9 \text{ fb}^{-1}$ , the required luminosity to probe  $\lambda_{hAA} \approx 0.1$  GeV in the CMS channel would require almost  $35.9 \times 10^4 \text{ fb}^{-1}$  luminosity. Thus, our proposed method provides an improved limit in the region  $m_A \leq \frac{m_h}{2}$  considering 10% systematic uncertainty.

The potential scope for quality improvement in our analysis can be performed in two places. Firstly, the kinetic distributions, such as the invariant mass of  $2\ell^\pm + 2\tau^\mp$ , are generated at the LO, and only the overall cross section is scaled by NLO  $k$ -factors. This can be improved to the kinetic distribution at NLO. Secondly, we have used the simplified  $\tau$ -identification as implemented in `Delphes` which can be refined to more realistic  $\tau$  taggers. The `Delphes`  $\tau$ -tagger uses an efficiency-based implementation, i.e. an efficiency is used in the  $\tau$ -objects, and a misidentification rate is used for other objects to incorporate the effects of faking other objects as  $\tau$ -jets. In our analysis through `Delphes`, we have chosen a working point with efficiency as 60% and jet $\rightarrow$ tau misidentification probability as 1% [111]. With the latest ML-based `DeepTau` tagger [42], the misidentification rate can be reduced by a factor of two, especially for the jets coming from  $t\bar{t}$  sample. Therefore, a factor of four reduction in the dominant  $t\bar{t}$  background is possible, allowing for a two-fold improvement in the significance. Although a thorough analysis is required to quote a concrete number, a significant improvement is expected with the help of the state-of-the-art `DeepTau` tagger.

#### IV. SUMMARY AND CONCLUSION

The exotic decay modes of  $h$  into two on-shell pseudoscalars ( $A$ ) is a primary signature of a Type-X 2HDM whenever the decay is kinematically allowed. The CMS and ATLAS collaborations at the LHC have met with null results in these efforts in the search for  $h \rightarrow AA$  mostly in the  $4\tau$  channel, for  $m_A < 62.5$  GeV.

In this work, we have investigated, in the context of the collider signatures of  $h \rightarrow AA^{(*)}$  in  $4\tau$  channel. We show that it is possible to achieve visibility for one off-shell pseudoscalar if we look for the final state comprising two same-sign leptons along with two same-sign  $\tau$ -jets. In this

---

<sup>1</sup> This relation also assumes the denominator of the Eq. (5) changes negligibly since the 95% C.L. limit by CMS on the  $\text{BR}(h \rightarrow AA)$  is less than a few per cent.

channel, the SM background, as we show, can be strongly eliminated. The important feature of our proposal is that the probe is feasible for  $m_A > m_h/2$ , where one pseudoscalar is produced off-shell. The minimum  $hAA^*$  interaction strength that can be thus probed at the high-luminosity run of the LHC has been obtained for  $m_A$  all the way to 85 GeV. We present our results in terms of the potential discovery limit of the  $\lambda_{hAA}$  coupling at the  $2\sigma$  and  $3\sigma$ . We further have shown the potential improvement in the probe of  $hAA$  coupling for the pseudoscalar masses  $m_A < m_h/2$  at the LHC with  $1000 \text{ fb}^{-1}$  and  $3000 \text{ fb}^{-1}$  integrated luminosity. To achieve the probe of  $\lambda_{hAA}$  received with our strategy, the conventional searches would require approximately  $3.6 \times 10^5 \text{ fb}^{-1}$  integrated luminosity at a 14 TeV hadron collider.

## ACKNOWLEDGEMENTS

The authors are thankful to the High Performance Computing (HPC) Cluster (Kepler) facility provided by the Department of Physical Sciences at IISER Kolkata. S. S. thanks to the Council of Scientific and Industrial Research (CSIR) for funding this project.

- 
- [1] G.C. Branco, P.M. Ferreira, L. Lavoura, M.N. Rebelo, M. Sher and J.P. Silva, *Theory and phenomenology of two-Higgs-doublet models*, *Phys. Rept.* **516** (2012) 1 [[1106.0034](#)].
  - [2] G. Bhattacharyya and D. Das, *Scalar sector of two-Higgs-doublet models: A minireview*, *Pramana* **87** (2016) 40 [[1507.06424](#)].
  - [3] R. Aggleton, D. Barducci, N.-E. Bomark, S. Moretti and C. Shepherd-Themistocleous, *Review of LHC experimental results on low mass bosons in multi Higgs models*, *JHEP* **02** (2017) 035 [[1609.06089](#)].
  - [4] H. Davoudiasl, I.M. Lewis and M. Sullivan, *Good things to do with extra Higgs doublets*, in *Snowmass 2021*, 3, 2022 [[2203.01396](#)].
  - [5] I.P. Ivanov, *Building and testing models with extended Higgs sectors*, *Prog. Part. Nucl. Phys.* **95** (2017) 160 [[1702.03776](#)].
  - [6] T. Robens, *The THDMa Revisited*, *Symmetry* **13** (2021) 2341 [[2106.02962](#)].
  - [7] V.D. Barger, J.L. Hewett and R.J.N. Phillips, *New Constraints on the Charged Higgs Sector in Two Higgs Doublet Models*, *Phys. Rev. D* **41** (1990) 3421.
  - [8] Y. Grossman, *Phenomenology of models with more than two Higgs doublets*, *Nucl. Phys. B* **426** (1994) 355 [[hep-ph/9401311](#)].
  - [9] M. Aoki, S. Kanemura, K. Tsumura and K. Yagyu, *Models of Yukawa interaction in the two Higgs doublet model, and their collider phenomenology*, *Phys. Rev. D* **80** (2009) 015017 [[0902.4665](#)].



- [10] L. Wang, J.M. Yang and Y. Zhang, *Two-Higgs-doublet models in light of current experiments: a brief review*, *Commun. Theor. Phys.* **74** (2022) 097202 [2203.07244].
- [11] J. Cao, P. Wan, L. Wu and J.M. Yang, *Lepton-Specific Two-Higgs Doublet Model: Experimental Constraints and Implication on Higgs Phenomenology*, *Phys. Rev. D* **80** (2009) 071701 [0909.5148].
- [12] E.J. Chun, S. Dwivedi, T. Mondal and B. Mukhopadhyaya, *Reconstructing a light pseudoscalar in the Type-X Two Higgs Doublet Model*, *Phys. Lett. B* **774** (2017) 20 [1707.07928].
- [13] E.J. Chun, S. Dwivedi, T. Mondal, B. Mukhopadhyaya and S.K. Rai, *Reconstructing heavy Higgs boson masses in a type X two-Higgs-doublet model with a light pseudoscalar particle*, *Phys. Rev. D* **98** (2018) 075008 [1807.05379].
- [14] A. Dey and J. Lahiri, *Collider Signatures of Type-X 2HDM + scalar singlet dark matter at HL-LHC*, **2112.15536**.
- [15] ATLAS collaboration, *Observation of a new particle in the search for the Standard Model Higgs boson with the ATLAS detector at the LHC*, *Phys. Lett. B* **716** (2012) 1 [1207.7214].
- [16] CMS collaboration, *Observation of a New Boson at a Mass of 125 GeV with the CMS Experiment at the LHC*, *Phys. Lett. B* **716** (2012) 30 [1207.7235].
- [17] X.-F. Han, F. Wang, L. Wang, J.M. Yang and Y. Zhang, *Joint explanation of W-mass and muon  $g-2$  in the 2HDM\**, *Chin. Phys. C* **46** (2022) 103105 [2204.06505].
- [18] I. Baum, *Top quark rare decays in a two Higgs doublet model for the top*, M.Sc. Thesis, 11, 2007, [0711.1311].
- [19] T. Barakat, *The rare decay in the two-higgs doublet model*, *Journal of Physics G: Nuclear and Particle Physics* **24** (1998) 1903.
- [20] M. Misiak and M. Steinhauser, *Weak radiative decays of the B meson and bounds on  $M_{H^\pm}$  in the Two-Higgs-Doublet Model*, *Eur. Phys. J. C* **77** (2017) 201 [1702.04571].
- [21] B. Mukhopadhyaya, S. Samanta, T. Samui and R.K. Singh, *Novel signals for the type-X two-Higgs-doublet scenario at the Large Hadron Collider*, *Phys. Rev. D* **108** (2023) 075004 [2305.16403].
- [22] C.-T. Lu, L. Wu, Y. Wu and B. Zhu, *Electroweak precision fit and new physics in light of the W boson mass*, *Phys. Rev. D* **106** (2022) 035034 [2204.03796].
- [23] A. Dey, J. Lahiri and B. Mukhopadhyaya, *Muon  $g-2$  and a type-X two-Higgs-doublet scenario: Some studies in high-scale validity*, *Phys. Rev. D* **106** (2022) 055023 [2106.01449].
- [24] J.F. Gunion and H.E. Haber, *The CP conserving two Higgs doublet model: The Approach to the decoupling limit*, *Phys. Rev. D* **67** (2003) 075019 [hep-ph/0207010].
- [25] S. Karmakar and S. Rakshit, *Alignment Limit in 2HDM: Robustness put to test*, *JHEP* **09** (2018) 142 [1802.03366].
- [26] L. Evans and P. Bryant, eds., *LHC Machine*, *JINST* **3** (2008) S08001.
- [27] W.-s. Hou, R. Jain and C. Kao, *Prospects for extra Higgs boson search via  $pp \rightarrow H, A \rightarrow \tau\mu, \tau\tau$  at the high luminosity Large Hadron Collider*, *Eur. Phys. J. C* **83** (2023) 1112 [2202.04336].

- [28] A. Adhikary, S. Banerjee, R.K. Barman, B. Batell, B. Bhattacharjee, C. Bose et al., *Prospects for exotic  $h \rightarrow 4\tau$  decays in single and di-Higgs boson production at the LHC and future hadron colliders*, *Phys. Rev. D* **109** (2024) 055008 [2211.07674].
- [29] D. Contardo, M. Klute, J. Mans, L. Silvestris and J. Butler, *Technical Proposal for the Phase-II Upgrade of the CMS Detector*, *Tech. Rep.*, Geneva (2015).
- [30] CMS collaboration, *The Phase-2 Upgrade of the CMS Level-1 Trigger*, *Tech. Rep.*, CERN, Geneva (2020).
- [31] Y. Ma, A. Arhrib, S. Moretti, S. Semmlali, Y. Wang and Q.S. Yan, *Analysis of the  $gg \rightarrow H \rightarrow hh \rightarrow 4\tau$  process in the 2HDM lepton specific model at the LHC*, 2401.07289.
- [32] ATLAS collaboration, *Search for Higgs boson decays to beyond-the-Standard-Model light bosons in four-lepton events with the ATLAS detector at  $\sqrt{s} = 13$  TeV*, *JHEP* **06** (2018) 166 [1802.03388].
- [33] CMS collaboration, *A search for pair production of new light bosons decaying into muons in proton-proton collisions at 13 TeV*, *Phys. Lett. B* **796** (2019) 131 [1812.00380].
- [34] ATLAS collaboration, *Search for the Higgs boson produced in association with a vector boson and decaying into two spin-zero particles in the  $H \rightarrow aa \rightarrow 4b$  channel in  $pp$  collisions at  $\sqrt{s} = 13$  TeV with the ATLAS detector*, *JHEP* **10** (2018) 031 [1806.07355].
- [35] ATLAS collaboration, *Search for Higgs boson decays into two new low-mass spin-0 particles in the  $4b$  channel with the ATLAS detector using  $pp$  collisions at  $\sqrt{s} = 13$  TeV*, *Phys. Rev. D* **102** (2020) 112006 [2005.12236].
- [36] CMS collaboration, *Search for an exotic decay of the Higgs boson to a pair of light pseudoscalars in the final state with two  $b$  quarks and two  $\tau$  leptons in proton-proton collisions at  $\sqrt{s} = 13$  TeV*, *Phys. Lett. B* **785** (2018) 462 [1805.10191].
- [37] ATLAS collaboration, *Search for Higgs bosons decaying to  $aa$  in the  $\mu\mu\tau\tau$  final state in  $pp$  collisions at  $\sqrt{s} = 8$  TeV with the ATLAS experiment*, *Phys. Rev. D* **92** (2015) 052002 [1505.01609].
- [38] CMS collaboration, *Search for light bosons in decays of the 125 GeV Higgs boson in proton-proton collisions at  $\sqrt{s} = 8$  TeV*, *JHEP* **10** (2017) 076 [1701.02032].
- [39] CMS collaboration, *Search for an exotic decay of the Higgs boson to a pair of light pseudoscalars in the final state of two muons and two  $\tau$  leptons in proton-proton collisions at  $\sqrt{s} = 13$  TeV*, *JHEP* **11** (2018) 018 [1805.04865].
- [40] CMS collaboration, *Search for light pseudoscalar boson pairs produced from decays of the 125 GeV Higgs boson in final states with two muons and two nearby tracks in  $pp$  collisions at  $\sqrt{s} = 13$  TeV*, *Phys. Lett. B* **800** (2020) 135087 [1907.07235].
- [41] CMS collaboration, *Search for a light pseudoscalar Higgs boson in the boosted  $\mu\mu\tau\tau$  final state in proton-proton collisions at  $\sqrt{s} = 13$  TeV*, *JHEP* **08** (2020) 139 [2005.08694].
- [42] CMS collaboration, *Identification of hadronic tau lepton decays using a deep neural network*, *JINST* **17** (2022) P07023 [2201.08458].

- [43] L. Wang and X.-F. Han, *A light pseudoscalar of 2HDM confronted with muon  $g-2$  and experimental constraints*, *JHEP* **05** (2015) 039 [[1412.4874](#)].
- [44] V. Ilisie, *New Barr-Zee contributions to  $(g - 2)_\mu$  in two-Higgs-doublet models*, *JHEP* **04** (2015) 077 [[1502.04199](#)].
- [45] T. Abe, R. Sato and K. Yagyu, *Lepton-specific two Higgs doublet model as a solution of muon  $g - 2$  anomaly*, *JHEP* **07** (2015) 064 [[1504.07059](#)].
- [46] N. Ghosh and J. Lahiri, *Revisiting a generalized two-Higgs-doublet model in light of the muon anomaly and lepton flavor violating decays at the HL-LHC*, *Phys. Rev. D* **103** (2021) 055009 [[2010.03590](#)].
- [47] N. Ghosh and J. Lahiri, *Generalized 2HDM with wrong-sign lepton-Yukawa coupling, in light of  $g_\mu - 2$  and lepton flavor violation at the future LHC*, *Eur. Phys. J. C* **81** (2021) 1074 [[2103.10632](#)].
- [48] A. Jueid, J. Kim, S. Lee and J. Song, *Type-X two-Higgs-doublet model in light of the muon  $g-2$ : Confronting Higgs boson and collider data*, *Phys. Rev. D* **104** (2021) 095008 [[2104.10175](#)].
- [49] S. Iguro, T. Kitahara, M.S. Lang and M. Takeuchi, *Current status of the muon  $g-2$  interpretations within two-Higgs-doublet models*, *Phys. Rev. D* **108** (2023) 115012 [[2304.09887](#)].
- [50] MUON  $G-2$  collaboration, *Measurement of the Positive Muon Anomalous Magnetic Moment to 0.20 ppm*, *Phys. Rev. Lett.* **131** (2023) 161802 [[2308.06230](#)].
- [51] T. Aoyama et al., *The anomalous magnetic moment of the muon in the Standard Model*, *Phys. Rept.* **887** (2020) 1 [[2006.04822](#)].
- [52] FERMILAB LATTICE, LATTICE-HPQCD, MILC collaboration, *Strong-Isospin-Breaking Correction to the Muon Anomalous Magnetic Moment from Lattice QCD at the Physical Point*, *Phys. Rev. Lett.* **120** (2018) 152001 [[1710.11212](#)].
- [53] D. Giusti, F. Sanfilippo and S. Simula, *Light-quark contribution to the leading hadronic vacuum polarization term of the muon  $g - 2$  from twisted-mass fermions*, *Phys. Rev. D* **98** (2018) 114504 [[1808.00887](#)].
- [54] D. Giusti, V. Lubicz, G. Martinelli, F. Sanfilippo and S. Simula, *Electromagnetic and strong isospin-breaking corrections to the muon  $g - 2$  from Lattice QCD+QED*, *Phys. Rev. D* **99** (2019) 114502 [[1901.10462](#)].
- [55] PACS collaboration, *Hadronic vacuum polarization contribution to the muon  $g - 2$  with 2+1 flavor lattice QCD on a larger than  $(10 \text{ fm})^4$  lattice at the physical point*, *Phys. Rev. D* **100** (2019) 034517 [[1902.00885](#)].
- [56] FERMILAB LATTICE, LATTICE-HPQCD, MILC collaboration, *Hadronic-vacuum-polarization contribution to the muon's anomalous magnetic moment from four-flavor lattice QCD*, *Phys. Rev. D* **101** (2020) 034512 [[1902.04223](#)].
- [57] A. Gérardin, M. Cè, G. von Hippel, B. Hörz, H.B. Meyer, D. Mohler et al., *The leading hadronic contribution to  $(g - 2)_\mu$  from lattice QCD with  $N_f = 2 + 1$  flavours of  $O(a)$  improved Wilson quarks*, *Phys. Rev. D* **100** (2019) 014510 [[1904.03120](#)].

- [58] T. Blum, N. Christ, M. Hayakawa, T. Izubuchi, L. Jin, C. Jung et al., *Hadronic Light-by-Light Scattering Contribution to the Muon Anomalous Magnetic Moment from Lattice QCD*, *Phys. Rev. Lett.* **124** (2020) 132002 [[1911.08123](#)].
- [59] S. Borsanyi et al., *Leading hadronic contribution to the muon magnetic moment from lattice QCD*, *Nature* **593** (2021) 51 [[2002.12347](#)].
- [60] M. Cè et al., *Window observable for the hadronic vacuum polarization contribution to the muon  $g-2$  from lattice QCD*, *Phys. Rev. D* **106** (2022) 114502 [[2206.06582](#)].
- [61] EXTENDED TWISTED MASS collaboration, *Lattice calculation of the short and intermediate time-distance hadronic vacuum polarization contributions to the muon magnetic moment using twisted-mass fermions*, *Phys. Rev. D* **107** (2023) 074506 [[2206.15084](#)].
- [62] E.-H. Chao, H.B. Meyer and J. Parrino, *Coordinate-space calculation of the window observable for the hadronic vacuum polarization contribution to  $(g-2)_\mu$* , *Phys. Rev. D* **107** (2023) 054505 [[2211.15581](#)].
- [63] M. Davier, A. Hoecker, B. Malaescu and Z. Zhang, *A new evaluation of the hadronic vacuum polarisation contributions to the muon anomalous magnetic moment and to  $\alpha(m_Z^2)$* , *Eur. Phys. J. C* **80** (2020) 241 [[1908.00921](#)].
- [64] A. Keshavarzi, D. Nomura and T. Teubner,  *$g - 2$  of charged leptons,  $\alpha(M_Z^2)$ , and the hyperfine splitting of muonium*, *Phys. Rev. D* **101** (2020) 014029 [[1911.00367](#)].
- [65] CMD-3 collaboration, *Measurement of the  $e^+e^- \rightarrow \pi^+\pi^-$  cross section from threshold to 1.2 GeV with the CMD-3 detector*, *Phys. Rev. D* **109** (2024) 112002 [[2302.08834](#)].
- [66] M. Sher, *Flavor-changing neutral currents in the Higgs sector*, *Mod. Phys. Lett. A* **37** (2022) 2230011 [[2207.06771](#)].
- [67] F. Arco, S. Heinemeyer and M.J. Herrero, *Sensitivity and constraints to the 2HDM soft-breaking  $Z_2$  parameter  $m_{12}$* , *Phys. Lett. B* **835** (2022) 137548 [[2207.13501](#)].
- [68] I.P. Ivanov, *Minkowski space structure of the higgs potential in the two-higgs-doublet model*, *Phys. Rev. D* **75** (2007) 035001.
- [69] S. Chang, S.K. Kang, J.-P. Lee and J. Song, *Higgs potential and hidden light Higgs scenario in two Higgs doublet models*, *Phys. Rev. D* **92** (2015) 075023 [[1507.03618](#)].
- [70] A. Arhrib, *Unitarity constraints on scalar parameters of the standard and two Higgs doublets model*, in *Workshop on Noncommutative Geometry, Superstrings and Particle Physics*, 12, 2000, [hep-ph/0012353](#).
- [71] I.F. Ginzburg and I.P. Ivanov, *Tree-level unitarity constraints in the most general 2HDM*, *Phys. Rev. D* **72** (2005) 115010 [[hep-ph/0508020](#)].
- [72] MUON G-2 collaboration, *Final Report of the Muon E821 Anomalous Magnetic Moment Measurement at BNL*, *Phys. Rev. D* **73** (2006) 072003 [[hep-ex/0602035](#)].
- [73] P. Bechtle, S. Heinemeyer, T. Klingl, T. Stefaniak, G. Weiglein and J. Wittbrodt, *HiggsSignals-2: Probing new physics with precision Higgs measurements in the LHC 13 TeV era*, *Eur. Phys. J. C* **81**

- (2021) 145 [2012.09197].
- [74] H. Bahl, T. Biekötter, S. Heinemeyer, C. Li, S. Paasch, G. Weiglein et al., *HiggsTools: BSM scalar phenomenology with new versions of HiggsBounds and HiggsSignals*, *Comput. Phys. Commun.* **291** (2023) 108803 [2210.09332].
- [75] ATLAS collaboration, *Search for Higgs boson decays into a pair of light bosons in the  $b\bar{b}\mu\mu$  final state in  $pp$  collision at  $\sqrt{s} = 13$  TeV with the ATLAS detector*, *Phys. Lett. B* **790** (2019) 1 [1807.00539].
- [76] CMS collaboration, *Search for an exotic decay of the Higgs boson to a pair of light pseudoscalars in the final state with two muons and two  $b$  quarks in  $pp$  collisions at 13 TeV*, *Phys. Lett. B* **795** (2019) 398 [1812.06359].
- [77] CMS collaboration, *Search for a new scalar resonance decaying to a pair of  $Z$  bosons in proton-proton collisions at  $\sqrt{s} = 13$  TeV*, *JHEP* **06** (2018) 127 [1804.01939].
- [78] ATLAS collaboration, *Combination of searches for heavy resonances decaying into bosonic and leptonic final states using  $36 \text{ fb}^{-1}$  of proton-proton collision data at  $\sqrt{s} = 13$  TeV with the ATLAS detector*, *Phys. Rev. D* **98** (2018) 052008 [1808.02380].
- [79] CMS collaboration, *Search for a heavy Higgs boson decaying to a pair of  $W$  bosons in proton-proton collisions at  $\sqrt{s} = 13$  TeV*, *JHEP* **03** (2020) 034 [1912.01594].
- [80] ATLAS collaboration, *Search for pair production of Higgs bosons in the  $b\bar{b}b\bar{b}$  final state using proton-proton collisions at  $\sqrt{s} = 13$  TeV with the ATLAS detector*, *JHEP* **01** (2019) 030 [1804.06174].
- [81] ATLAS collaboration, *Search for Higgs boson pair production in the  $\gamma\gamma WW^*$  channel using  $pp$  collision data recorded at  $\sqrt{s} = 13$  TeV with the ATLAS detector*, *Eur. Phys. J. C* **78** (2018) 1007 [1807.08567].
- [82] CMS collaboration, *Combination of searches for Higgs boson pair production in proton-proton collisions at  $\sqrt{s} = 13$  TeV*, *Phys. Rev. Lett.* **122** (2019) 121803 [1811.09689].
- [83] P. Bechtle, D. Dercks, S. Heinemeyer, T. Klingl, T. Stefaniak, G. Weiglein et al., *HiggsBounds-5: Testing Higgs Sectors in the LHC 13 TeV Era*, *Eur. Phys. J. C* **80** (2020) 1211 [2006.06007].
- [84] M.E. Peskin and T. Takeuchi, *Estimation of oblique electroweak corrections*, *Phys. Rev. D* **46** (1992) 381.
- [85] ALEPH, DELPHI, L3, OPAL, SLD, LEP ELECTROWEAK WORKING GROUP, SLD ELECTROWEAK GROUP, SLD HEAVY FLAVOUR GROUP collaboration, *Precision electroweak measurements on the  $Z$  resonance*, *Phys. Rept.* **427** (2006) 257 [hep-ex/0509008].
- [86] PARTICLE DATA GROUP collaboration, *Review of Particle Physics*, *PTEP* **2020** (2020) 083C01.
- [87] LHC HIGGS CROSS SECTION WORKING GROUP collaboration, *Handbook of LHC Higgs Cross Sections: 1. Inclusive Observables*, **1101.0593**.
- [88] A. Denner, S. Heinemeyer, I. Puljak, D. Rebuszi and M. Spira, *Standard Model Higgs-Boson Branching Ratios with Uncertainties*, *Eur. Phys. J. C* **71** (2011) 1753 [1107.5909].

- [89] S. Dittmaier et al., *Handbook of LHC Higgs Cross Sections: 2. Differential Distributions*, [1201.3084](#).
- [90] LHC HIGGS CROSS SECTION WORKING GROUP collaboration, *Handbook of LHC Higgs Cross Sections: 3. Higgs Properties*, [1307.1347](#).
- [91] LHC HIGGS CROSS SECTION WORKING GROUP collaboration, *Handbook of LHC Higgs Cross Sections: 4. Deciphering the Nature of the Higgs Sector*, [1610.07922](#).
- [92] A. Djouadi, J. Kalinowski and M. Spira, *HDECAY: A Program for Higgs boson decays in the standard model and its supersymmetric extension*, *Comput. Phys. Commun.* **108** (1998) 56 [[hep-ph/9704448](#)].
- [93] HDECAY collaboration, *HDECAY: Twenty<sub>++</sub> years after*, *Comput. Phys. Commun.* **238** (2019) 214 [[1801.09506](#)].
- [94] A. Bredenstein, A. Denner, S. Dittmaier and M.M. Weber, *Precise predictions for the Higgs-boson decay  $H \rightarrow WW/ZZ \rightarrow 4$  leptons*, *Phys. Rev. D* **74** (2006) 013004 [[hep-ph/0604011](#)].
- [95] A. Bredenstein, A. Denner, S. Dittmaier and M.M. Weber, *Precision calculations for the Higgs decays  $H \rightarrow ZZ/WW \rightarrow 4$  leptons*, *Nucl. Phys. B Proc. Suppl.* **160** (2006) 131 [[hep-ph/0607060](#)].
- [96] A. Bredenstein, A. Denner, S. Dittmaier and M.M. Weber, *Radiative corrections to the semileptonic and hadronic Higgs-boson decays  $H \rightarrow WW / ZZ \rightarrow 4$  fermions*, *JHEP* **02** (2007) 080 [[hep-ph/0611234](#)].
- [97] ATLAS collaboration, *Electron efficiency measurements with the ATLAS detector using 2012 LHC proton-proton collision data*, *Eur. Phys. J. C* **77** (2017) 195 [[1612.01456](#)].
- [98] CMS collaboration, *Muon identification using multivariate techniques in the CMS experiment in proton-proton collisions at  $\sqrt{s} = 13$  TeV*, *JINST* **19** (2024) P02031 [[2310.03844](#)].
- [99] F. Staub, *SARAH 4 : A tool for (not only SUSY) model builders*, *Comput. Phys. Commun.* **185** (2014) 1773 [[1309.7223](#)].
- [100] W. Porod and F. Staub, *SPheno 3.1: Extensions including flavour, CP-phases and models beyond the MSSM*, *Comput. Phys. Commun.* **183** (2012) 2458 [[1104.1573](#)].
- [101] J. Alwall, R. Frederix, S. Frixione, V. Hirschi, F. Maltoni, O. Mattelaer et al., *The automated computation of tree-level and next-to-leading order differential cross sections, and their matching to parton shower simulations*, *JHEP* **07** (2014) 079 [[1405.0301](#)].
- [102] C. Bierlich et al., *A comprehensive guide to the physics and usage of PYTHIA 8.3*, *SciPost Phys. Codeb.* **2022** (2022) 8 [[2203.11601](#)].
- [103] DELPHES 3 collaboration, *DELPHES 3, A modular framework for fast simulation of a generic collider experiment*, *JHEP* **02** (2014) 057 [[1307.6346](#)].
- [104] M. Cacciari, G.P. Salam and G. Soyez, *The anti- $k_t$  jet clustering algorithm*, *JHEP* **04** (2008) 063 [[0802.1189](#)].
- [105] R. Frederix and S. Frixione, *Merging meets matching in MC@NLO*, *JHEP* **12** (2012) 061 [[1209.6215](#)].

- [106] A. Kardos, Z. Trocsanyi and C. Papadopoulos, *Top quark pair production in association with a Z-boson at NLO accuracy*, *Phys. Rev. D* **85** (2012) 054015 [[1111.0610](#)].
- [107] S. von Buddenbrock, R. Ruiz and B. Mellado, *Anatomy of inclusive  $t\bar{t}W$  production at hadron colliders*, *Phys. Lett. B* **811** (2020) 135964 [[2009.00032](#)].
- [108] M. Czakon, P. Fiedler and A. Mitov, *Total Top-Quark Pair-Production Cross Section at Hadron Colliders Through  $O(\alpha_S^4)$* , *Phys. Rev. Lett.* **110** (2013) 252004 [[1303.6254](#)].
- [109] M. Grazzini, S. Kallweit, D. Rathlev and M. Wiesemann,  *$W^\pm Z$  production at hadron colliders in NNLO QCD*, *Phys. Lett. B* **761** (2016) 179 [[1604.08576](#)].
- [110] F. Cascioli, T. Gehrmann, M. Grazzini, S. Kallweit, P. Maierhöfer, A. von Manteuffel et al.,  *$ZZ$  production at hadron colliders in NNLO QCD*, *Phys. Lett. B* **735** (2014) 311 [[1405.2219](#)].
- [111] CMS collaboration, *Performance of reconstruction and identification of  $\tau$  leptons decaying to hadrons and  $\nu_\tau$  in  $pp$  collisions at  $\sqrt{s} = 13$  TeV*, *JINST* **13** (2018) P10005 [[1809.02816](#)].